HHS Public Access

Author manuscript

Proteomics. Author manuscript; available in PMC 2017 April 01.

Published in final edited form as:

Proteomics. 2016 April ; 16(8): 1271–1279. doi:10.1002/pmic.201500375.

Evaluation of Quantum dot immunofluorescence and a digital CMOS imaging system as an alternative to conventional organic fluorescence dyes and laser scanning for quantifying protein microarrays

Aarti Jain[1,#], **Omid Taghavian**[1,#], **Derek Vallejo**[2], **Emmanuel Dotsey**[1], **Dan Schwartz**[3], **Florian G. Bell**[3], **Chad Greef**[3], **D. Huw Davies**[1], **Jennipher Grudzien**[3], **Abraham P. Lee**[2], **Philip Felgner**[1], and **Li Liang**[1,*]

[1]Department of Medicine, division of infectious diseases, University of California Irvine, Irvine CA 92697

[2]Department of Biomedical Engineering, University of California Irvine, Irvine, USA 92697

[3]Grace Bio-Labs, Inc., 325 SW Cyber Drive, Bend, OR 97702

Abstract

Organic fluorescent dyes are widely used for the visualization of bound antibody in a variety of immunofluorescence assays. However, the detection equipment is often expensive, fragile and hard to deploy widely. Quantum dots (Qdot®) are nanocrystals made of semiconductor materials that emit light at different wavelengths according to the size of the crystal, with increased brightness and stability. Here we have evaluated a small benchtop 'personal' optical imager (ArrayCAM™) developed for quantification of protein arrays probed by Qdot -based indirect immunofluorescence. The aim was to determine if the Qdot imager system provides equivalent data to the conventional organic dye-labelled antibody/laser scanner system. To do this, duplicate proteome microarrays of Vaccinia virus, *Brucella melitensis* and *Plasmodium falciparum* were probed with identical samples of immune sera, and IgG, IgA and IgM profiles visualized using biotinylated secondary antibodies followed by a tertiary reagent of streptavidin coupled to either P3 (an organic cyanine dye typically used for microarrays) or Q800 (Qdot). The data show excellent correlation for all samples tested (R>0.8) with no significant change of antibody reactivity profiles. We conclude that Qdot detection provides data equivalent to that obtained using conventional organic dye detection. The portable imager offers an economical, more robust and deployable alternative to conventional laser array scanners.

*Correspondence should be sent to Dr. Li Liang lliang3@uci.edu, 376F MedSurge II, Dept. of Medicine, University of California Irvine, Irvine, CA 92697-1275. Phone: 949-824-7368. Fax: 949-824-0481.

#These authors contributed equally to this work

Conflict of Financial Interest

FB, JG, DS and CG are employees of Grace Bio-Labs, Inc. DHD and PLF disclose a financial interest in Antigen Discovery Inc., which has licensed a protein microarray technology. DHD, PLF and the University of California, Irvine may financially benefit from this interest if the company is successful in marketing its products that are related to this research. The terms of this arrangement have been reviewed and approved by the University of California, Irvine, in accordance with its conflict of interest policies.

Keywords

protein microarray; proteome; Quantum dots; diagnostics; antibody

Introduction

Quantum dots (Qdot®) are becoming popular tools as fluorescence probes in the field of biology. Qdots are quantum nanocrystals made of semiconductor materials that emit light at different wavelengths according to the size of the crystal. Due to their superior brightness and stability, and their broad excitation curve but narrow emission curves [1–6], Qdots have been commonly utilized in areas such as single-molecule detection and tracking, fluorescence resonance energy transfer (FRET), and tissue imaging [7–12].

Organic fluorescent dyes are widely used for the visualization of bound antibody in a variety of immunofluorescence assays and imaging applications, including fluorescence microscopy, flow cytometry, and protein and nucleic acid microarrays. Despite being widely established, traditional organic dyes do not offer the flexibility required to address all the needs of modern immunofluorescence applications. Moreover, the detection equipment required is often expensive and fragile and difficult to deploy worldwide [13, 14]. In the context of microarrays, recent developments in image capturing technology have also meant that traditional scanners are being replaced by simpler and more robust optical imaging systems that are more deployable than conventional laser scanners.

In this protein microarray study we evaluated a ‘personal’ array imager system (ArrayCAM™ from Grace Bio-Labs, Bend, OR) [15] and Qdot-based visualization of bound secondary antibodies as an alternative to organic fluorophores and conventional laser scanning. The imager uses a 405nm diode laser to excite bound Qdot-labelled probe and captures a high resolution fluorescence image using a digital camera. The protein microarray slides of Vaccinia virus, *Brucella melitensis* and *Plasmodium falciparum* were probed with identical serum samples and visualized using biotinylated secondary antibodies followed by a tertiary reagent of streptavidin coupled to either a conventional organic dye (P3) or Q800 (Qdot). We observed that Qdot detection provides equivalent data to that obtained using P3 detection. The personal imager captures and processes the image in less than a minute offers a robust and deployable alternative to conventional laser array scanners which take several minutes per slide.

Material and methods

Sera

Human Brucellosis sera were obtained from three patients infected with *B. melitensis* biovar 1 in Lima, Peru, as described previously [16, 17]. These patients were confirmed to have acute brucellosis by positive culture, positive Rose Bengal test and by tube agglutination tests titers >1/160.

Malaria samples were obtained from *P. falciparum* exposed individuals in Kalifabougou, Mali, and Kenya as described previously [18, 19]. Samples from *P. falciparum*-exposed

individuals in Papua New Guinea (PNG) were provided by Dr. James Kazura at Case Western Reserve University.

Vaccinia virus-specific sera were obtained from UK healthcare workers vaccinated in December 2002 against smallpox using Lister/Elstree vaccine (Swiss Serum Institute, Beme, Switzerland, batch number 84430 and 84431) [2].

Mouse monoclonal antibody against *P. falciparum* apical membrane protein-1 (AMA1) (Catalog # MRA-481A), and rabbit antisera against *P. falciparum* Merozoite Surface Protein 2 (MSP2) (Catalog # MRA-318) and MSP5 [20] (Catalog # MRA-320) were all obtained from BEI Resources (Manassas, VA).

Protein array construction

All ORFs from *Brucella melitensis* (*BM*) 16 M, Vaccinia virus (VACV) strain WR, and *Plasmodium falciparum* (*Pf*) 3D7 were identified, amplified and cloned using a high-throughput PCR and recombination cloning method described previously [16, 17, 21]. The *P. falciparum* array (Pf1000) was purchased from Antigen Discovery Inc., (Irvine, CA) and comprised 1087 exon products cloned from genomic DNA. Exons larger than 3kb were cloned in frame into multiple overlapping fragments. The protein targets on this array were down-selected from larger microarray studies [3, 22, 23] based on immunogenicity to humans. Full proteome *Brucella* and VACV-WR arrays were used in this study, displaying 3198 and 224 polypeptides, respectively.

Microarrays were fabricated as described [21]. Briefly, plasmids were expressed at 24 °C for 16 h in *E. coli*-based *in vitro* transcription/translation (IVTT) reactions (Expressway Maxi kits from 5 Prime, Gaithersburg, MD). For microarrays, 10 μL of reaction mixture was mixed with 3.3 μL 0.2% Tween 20 to give a final concentration of 0.05% Tween 20, and printed onto nitrocellulose coated glass AVID slides (Grace Bio-Labs, Inc., Bend, OR) using an Omni Grid 100 microarray printer (Genomic Solutions). Protein expression was monitored using antibodies against N-terminal polyhistidine (HIS) and C-terminal influenza hemagglutinin (HA) epitope tags engineered into each protein.

Microarray probing

Serum samples were diluted 1:100 in protein array blocking buffer (Maine Manufacturing, Sanford, ME) supplemented with *E. coli* lysate (GenScript, Piscataway, NJ) to a final concentration of 10mg/ml, and pre-incubated at room temperature (RT) for 30 min. Concurrently, arrays were rehydrated in blocking buffer (without lysate) for 30 min. Blocking buffer was removed, and arrays were probed with pre-incubated serum samples using sealed chambers to ensure no cross-contamination of sample between pads. Arrays were incubated over-night at 4 °C with gentle agitation. Arrays were then washed at RT five times with TBS-0.05% Tween 20 (T-TBS), followed by incubation with biotin-conjugated goat anti-human IgG/ IgM/ IgA (Jackson ImmunoResearch, West Grove, PA) diluted 1:200 in blocking buffer for 1 h at RT. Mouse monoclonal AMA1 antibody and Rabbit antisera against MSP2 or MSP5 antibodies were incubated with Pf1000 arrays in serial dilutions overnight at 4 °C with agitation, followed by biotin-conjugated anti mouse secondary antibody for AMA1, or biotin-conjugated anti-rabbit secondary antibody for MSP2 or MSP5

(BioLegend, San Diego, CA). After incubation in secondary antibodies, arrays were then washed three times with T-TBS, followed by incubation with either streptavidin-conjugated SureLight® P3 (Columbia Biosciences, Frederick, MD) or QDot® 800 Streptavidin Conjugate (conjugated with approximately 5 to 10 streptavidins per Qdot nanocrystal, nanometer-scale crystal of a semiconductor material (CdSe) coated with an additional semiconductor shell (ZnS), from Molecular Probes by Life Technologies, Eugene, Oregon, USA, catalog # Q10173MP) for 45 min at RT protected from light. Arrays were washed three times with T-TBS, and once with water. Chips were air dried by centrifugation at 1,000 g for 5 min and scanned on a Genepix 4200AL scanner (Molecular Devices, Sunnyvale, CA) for SureLight® P3 or ArrayCam™ 400-S Microarray Imaging System from Grace Bio-Labs (Bend, OR) for QDot. Spot and background intensities were measured using an annotated grid (.gal) file. Settings for the GenePix scanner were optimized for each type of arrays. Laser power (LP) has been set at 100%, photomultiplier tube (PMT) has been set for IgG/M/A subtypes for different arrays, at 310/300/310PMT for Pf1000 arrays, 330/330/330 PMT/ for VACV –WR arrays, and 310/310/310 PMT for Brucella arrays. The ArrayCam™ settings were set at 50 gain, and the exposure time in milliseconds (ms) was optimized for IgG/M/A subtypes (50/50/50ms for Pf1000 arrays, 100/100/100ms for VACV-WR arrays, and 50/50/50ms for Brucella arrays).

	Genepix (LP 100%)			Arraycam (Gain 50)		
	IgG	IgM	IgA	IgG	IgM	IgA
Malaria	310 PMT	300 PMT	310 PMT	50 ms	50 ms	50 ms
Vaccinia	330 PMT	330 PMT	330 PMT	100 ms	100 ms	100 ms
Brucella	310 PMT	310 PMT	310 PMT	50 ms	50 ms	50 ms

Data Analysis

Microarray spot intensities were quantified using ScanArrayExpress software (Perkin Elmer) or software ArrayCAM™ (Grace Bio-Labs) utilizing automatic local background subtraction for each spot. The generated signal intensity values were considered raw values. *E.coli* background signals from IVTT reaction without DNA template (no DNA control) were subtracted from raw values. The data were normalized by dividing the IVTT protein spot raw intensity by the sample specific median of the IVTT control spots (no DNA control). This fold-over control (FOC) approach provides a relative measure of the specific antibody binding over the IVTT background. This FOC normalization approach was used for comparing individual samples detected with organic dye or Qdot as shown in Supplmentary figure 1. Differential analyses of the log2-transfomed data were performed using a Bayes-regularized *t* test for protein arrays [24–27]. Differences were considered significant with Benjamini Hochberg corrected p-values<0.05 [28]. Antigens are considered reactive when mean reactivity (after removal of *E.coli* background) among exposed individuals is greater than 2 times of standard deviations above the mean of the no DNA controls. Z-scores of signal intensity were calculated as the number of standard deviations above the mean signal intensity (after removal of *E.coli* background) of the unexposed USA

control group. Mann-whitney p values were calculated for comparing distribution of raw signals among different detection methods.

Scatterplots were graphed with raw values with *E.coli* background signals from control spots of IVTT reaction without DNA template (*no DNA* spots) subtracted. Titration curves and dissociation constant (Kd) calculation for antibodies were also generated from raw data with *E.coli* background signals removed, using GraphPad Prism (Version 4.0, GraphPad Software Inc., San Diego, USA).

Results

Direct comparison between Qdot and P3 detection for IgG, IgA and IgM

To compare the results obtained with the conventional organic dye and Qdot detection, arrays were probed with human samples from malaria and brucellosis cases, and from smallpox vaccinees. The arrays were imaged for IgG, IgM and IgA reactivity using biotinylated secondary antibodies followed by streptavidin conjugated to either Qdot or SureLight® P3. After image capture as .tiff files in either GenePix or ArrayCam™ scanners, all images were quantified using ScanArray software. Representative images of probed Pf1000 arrays are shown in Figure 1A. Optimal settings for the GenePix scanner and ArrayCAM were used for each type of arrays, as described in the Methods. Maximum signal intensities for both ArrayCam™ and GenePix were the same, 65535 (2^{16}-1) on the 16-bit intensity scale. After equivalent settings were obtained, scatter plots were plotted with values from the conventional GenePix scanner on the y-axis, and the data from the ArrayCam™ on the x-axis (Figure 1BCD). Spot values were also normalized using a fold over no DNA control approach as described in Methods. The normalized values from both scanners were plotted in Supplementary figure 1. Overall, the R square values are above 0.8–0.9 for IgG, IgM, and IgA signals except for cases where fewer reactive IgM or IgA antigens were detected. Data for all the individual samples probed are compiled in Table 1.

Comparison of Qdot and SureLight® P3 on antibody profiling measurements

One particular aim of our protein microarray approach has been to discover antigens useful for serodiagnosis of infected patients from healthy controls [4, 12, 21, 29]. Thus, it is important to show equivalent differentially reactive antigen profiles when infected patients are compared with healthy controls. In addition to the 7 Kenyan *Pf* exposed samples, we also probed 6 USA naïve control samples on Pf1000 array, using either Qdot or SureLight® P3 detecting fluorophores. We first compared the antibody levels for all antigens (Figure 2A). The lower quartile signals (signals below quartile 1) among *Pf* exposed individuals detected with Qdot are significantly higher than that detected with P3 (p value <0.001) indicating that Qdots are more sensitive detecting weaker signals. Signals higher than the upper quartile (signals above quartile 3) were not significantly different.

The top 100 reactive antigens with highest average signal intensity in exposed individuals were selected from each method (Figure 2B, Supplementary Table 1), of which 81 were shared by each method. Out of these 119 top reactive antigens, 95 and 105 differentially reactive antigens were identified by Qdot or P3 detection, respectively, with 91 (83%) of

these differentially reactive antigens shared by each method. These differentially reactive antigens distinguish Plasmodium exposed patients from USA healthy controls with Benjamini Hochberg adjusted p value<0.05 (Figure 2)[28]. A further comparison showed that the top 400 reactive antigens identified from each method shared 87% of these antigens between each method. We calculated Z scores against USA control group within each method, and numbers of antigens with mean signals in *Pf* exposed individuals greater than 2 standard deviation of mean of USA controls (Z score>2) were identified. The percentages of antigens with Z score greater than 2 are 87% and 82%, from P3 and Qdot detection methods, respectively (supplementary figure 2). We conclude that these two detection methods generated similar lists of differentially reactive antigens, and Qdot detection does not significantly change the antibody profile compared to organic dye P3 detection.

Comparison of Qdot and P3 on antibody equilibrium binding measurements

To further compare the two detection systems we measured antibody binding constants by titrating one monoclonal antibody against AMA1 and two polyclonal antisera against MSP2 or MSP5 on Pf1000 arrays. Antibody titration curves (Figure 3) show that although the signal intensities at saturation for all antibodies were different, they all reached saturation at a range of 5 – 10 nM. The binding data was generated by titrating antibodies at five concentrations. To fit the experimental data, we employed one site specific binding model (nonlinear regression curve fitting analysis). The binding affinity of AMA1 detected with P3 (Kd=0.94 nM) is slightly lower compared with that of AMA1 detected with Qdot (Kd=0.87 nM). Binding affinity for MSP2-P3 (Kd=1.94nM) is also lower compared to that of MSP2-Q800 (Kd=1.55nM). Conversely, binding affinity for MSP5 detected with P3 (Kd= 0.50 nM) is slightly higher than that of MSP5 detected with Qdot (0.52 nM). Overall we conclude that binding constants determined by the two detection systems are equivalent.

Comparison of data acquired using ArrayCam vs ScanArrayExpress software

In all of the above comparisons, we compared organic dye P3 and Qdot fluorophore detection results by using the same ScanArrayExpress software. Next, we compared the data acquired using the quantification software supplied with the ArrayCam with that obtained using ScanArrayExpress. As shown in the scatterplot (Figure 4A), data obtained from a tiff image of a P3-labelled array acquired using ArrayCam and ScanArrayExpress software exhibit a perfect correlation with R^2=1.0 and slope of 0.99. Similarly, a tiff image of a Qdot-labelled array quantified in both software applications correlated well (R^2= 0.99, slope = 0.87).

Discussion

Quantum dots have been applied as fluorescence probes to many areas in the biological field, from *in vitro* immunofluorescence assays to *in vivo* trafficking. Qdots have superior optical properties that differentiate them from traditional organic dyes, such as extremely broad and intense absorption, and high fluorescence in the visible and near-infrared wavelengths [1, 13, 30–37]. Qdots have also been reported to show better photo stability over organic dyes for intense laser excitation or long scanning time [13]. Since Qdots have a

relatively broad excitation curve but narrow emission curves compared to organic fluorophores, they are more favored for multiplexed imaging studies [38].

Traditional organic molecules have been commercially available and well established as fluorescent probes for years in imaging applications, despite their non-optimum optical features [6, 39]. Organic fluorophores can be read in conventional confocal and non-confocal laser scanners which have been used for microarray studies in recent years. The Genepix laser scanner 4200AL used in this study has non-confocal optics designed for microarray imaging. The benefits of using non-confocal laser scanners may come from the findings that most of the non-specific background signal on a microarray slide is in the same focal plane as the array, and thus not reduced or benefited by confocal imaging. Moreover, whereas some confocal laser scanners have wide focal depth and may automatically adjust for optimal focal plane for various slides, others may have very narrow depth of field and may easily fluctuate away from optimal focal plane for slides with thick coating (www.moleculardevices.com) [5, 14]. Despite being commercially available everywhere, these traditional microarray scanners often are difficult to be deployed worldwide due to their weight, fragility, and high cost.

The ArrayCAM™ portable array imager tested here, uses a sensitive digital camera to capture microarray slide images resulting from diode-laser excitation of Qdot or dye fluorophores such as SYPRO® Ruby or Fast Green. The camera can detect weak signals from three dimensional coatings (www.gracebio.com). Currently the instrument is configured for four different emission wavelengths that allow up to 4 different labels to be quantified simultaneously (such as IgG, IgA and IgM). Shorter scanning time, and comparable high resolution at 10μM are two other characteristics of this instrument. Acquisition of slide images takes less than 1 minute with the digital camera, whereas laser scanners take 6–10 minutes per slide.

In this study, we aimed to evaluate if the digital camera/Qdot system provides equivalent data to conventional organic dye-labelled secondary antibody/laser scanner system used in our previous studies [4, 12, 21, 29]. To do this, the arrays were probed with serum samples according to our established protocol, with the exception that tertiary reagent was streptavidin conjugated to 800nm quantum-nanocrystals (Qdot) in place of the P3 organic fluorophore. We found that signal detection with P3 or Qdot in individual samples exhibited excellent correlations when quantified using the same (ScanArrayExpress) software or both ScanArrayExpress and ArrayCam™ software applications. Furthermore, after we compared the malaria patients and healthy controls, we found that the top 400 reactive antigens identified from each method shared 87% of these antigens between each method, and Qdot may be more sensitive in detecting lower signals on the array (Figure 2). We identified similar lists of differentially reactive antigens. Expanding the number of samples analyzed will be needed to confirm the specificity and accuracy of this analysis.

In this study, we applied a two- step detection method using streptavidin conjugated Qdot or organic P3. This is the first step towards applying the system for other protein microarray applications. Because of the discrete emission spectra of different Qdots, the Qdot system is well suited for multiplex testing. We are testing Qdot directly conjugated to various

secondary antibodies, to reduce the probing steps and allow for multiplex detection (ongoing work). We anticipate Qdot will provide increased benefit due to their long luminescence stability, high brightness or multi-color detections.

The results presented here demonstrate that Qdot fluorophore detection gives results equivalent to that obtained using conventional organic dye detection. These data will be an important factor for laboratories deciding to transition to a Qdot-based array detection system in place of more conventional organic fluorophores. Moreover, a portable instrument such as the ArrayCam™ evaluated here, or similar device that exploits Qdot detection and a modern digital camera, could easily be deployed in laboratory settings where purchase and maintenance of a more complex machine would be cost-prohibitive or impractical. Further cost reductions in scanning could be achieved in a simplified configuration (such as with a single emission filter) thereby offering an economical, robust and more deployable alternative to conventional laser array scanners, and providing new opportunities to individual labs wishing to probe and analyze their own microarrays independently in remote locations worldwide.

Supplementary Material

Refer to Web version on PubMed Central for supplementary material.

Acknowledgments

The work is supported by NIH grants R01AI095916 (PF) and U19AI089686 (PF), and Grace Bio-Labs funding number 202121.

We thank Grace Bio-Labs for providing technical support for the ArrayCam™. We would also like to thank Dr. Joseph Vinetz, University of California, San Diego, for providing Brucellosis serum samples; Dr. Geoff Smith, Cambridge, UK, for providing the Lister vaccine serum samples; Dr. Peter Crompton, National Institute of Health, for providing malaria samples from Kalifabougou in Mali; Dr. James Kazura, Case Western Reserve University for providing Papua New Guinea (PNG) samples and Kenyan malaria samples; and BEI Resources for providing mouse monoclonal AMA1 antibody (catalog # MRA-481A), rabbit antisera against MSP2 protein (Catalog # MRA-318, deposited by RL Coppel), and rabbit antisera against MSP5 protein (Catalog # MRA-320, deposited by RL Coppel).

References

1. Jiang W, Singhal A, Zheng JN, Wang C, Chan WCW. Optimizing the synthesis of red- to near-IR-emitting CdS-capped CdTexSe1-x alloyed quantum dots for biomedical imaging. Chem Mater. 2006; 18:4845–4854.
2. Putz MM, Midgley CM, Law M, Smith GL. Quantification of antibody responses against multiple antigens of the two infectious forms of Vaccinia virus provides a benchmark for smallpox vaccination. Nature medicine. 2006; 12:1310–1315.
3. Crompton PD, Kayala MA, Traore B, Kayentao K, et al. A prospective analysis of the Ab response to Plasmodium falciparum before and after a malaria season by protein microarray. Proc Natl Acad Sci U S A. 2010; 107:6958–6963. [PubMed: 20351286]
4. Felgner PL, Kayala MA, Vigil A, Burk C, et al. A Burkholderia pseudomallei protein microarray reveals serodiagnostic and cross-reactive antigens. Proc Natl Acad Sci U S A. 2009; 106:13499–13504. [PubMed: 19666533]
5. Sanderson MJ, Smith I, Parker I, Bootman MD. Fluorescence microscopy. Cold Spring Harbor protocols. 2014; 2014 pdb top071795.

6. Soper SA, Nutter HL, Keller RA, Davis LM, Shera EB. The Photophysical Constants of Several Fluorescent Dyes Pertaining to Ultrasensitive Fluorescence Spectroscopy. Photochem Photobiol. 1993; 57:972–977.
7. Alivisatos AP, Gu W, Larabell C. Quantum dots as cellular probes. Annual review of biomedical engineering. 2005; 7:55–76.
8. Medintz IL, Uyeda HT, Goldman ER, Mattoussi H. Quantum dot bioconjugates for imaging, labelling and sensing. Nat Mater. 2005; 4:435–446. [PubMed: 15928695]
9. Rosenthal SJ, Chang JC, Kovtun O, McBride JR, Tomlinson ID. Biocompatible quantum dots for biological applications. Chemistry & biology. 2011; 18:10–24. [PubMed: 21276935]
10. Pinaud F, Clarke S, Sittner A, Dahan M. Probing cellular events, one quantum dot at a time. Nat Methods. 2010; 7:275–285. [PubMed: 20354518]
11. Stanisavljevic M, Krizkova S, Vaculovicova M, Kizek R, Adam V. Quantum dots-fluorescence resonance energy transfer-based nanosensors and their application. Biosens Bioelectron. 2015; 74:562–574. [PubMed: 26188679]
12. Liang L, Juarez S, Nga TV, Dunstan S, et al. Immune profiling with a Salmonella Typhi antigen microarray identifies new diagnostic biomarkers of human typhoid. Scientific reports. 2013; 3:1043. [PubMed: 23304434]
13. Resch-Genger U, Grabolle M, Cavaliere-Jaricot S, Nitschke R, Nann T. Quantum dots versus organic dyes as fluorescent labels. Nat Methods. 2008; 5:763–775. [PubMed: 18756197]
14. Timlin JA. Scanning microarrays: current methods and future directions. Methods in enzymology. 2006; 411:79–98. [PubMed: 16939787]
15. Bell FG, et al. An Integrated Digital Imaging System and Microarray Mapping Software for Rapid Multiplexed Quantitation of Protein Microarray Immunoassays. 2015 In preparation.
16. Liang L, Leng D, Burk C, Nakajima-Sasaki R, et al. Large scale immune profiling of infected humans and goats reveals differential recognition of Brucella melitensis antigens. PLoS Negl Trop Dis. 2010; 4:e673. [PubMed: 20454614]
17. Liang L, Tan X, Juarez S, Villaverde H, et al. Systems Biology Approach Predicts Antibody Signature Associated with Brucella melitensis Infection in Humans. J Proteome Res. 2011; 10:4813–4824. [PubMed: 21863892]
18. Tran TM, Li S, Doumbo S, Doumtabe D, et al. An intensive longitudinal cohort study of Malian children and adults reveals no evidence of acquired immunity to Plasmodium falciparum infection. Clin Infect Dis. 2013; 57:40–47. [PubMed: 23487390]
19. Dent AE, Nakajima R, Liang L, Baum E, et al. Plasmodium falciparum Protein Microarray Antibody Profiles Correlate With Protection From Symptomatic Malaria in Kenya. J Infect Dis. 2015
20. Marshall VM, Tieqiao W, Coppel RL. Close linkage of three merozoite surface protein genes on chromosome 2 of Plasmodium falciparum. Mol Biochem Parasitol. 1998; 94:13–25. [PubMed: 9719507]
21. Davies DH, Liang X, Hernandez JE, Randall A, et al. Profiling the humoral immune response to infection by using proteome microarrays: high-throughput vaccine and diagnostic antigen discovery. Proc Natl Acad Sci U S A. 2005; 102:547–552. [PubMed: 15647345]
22. Trieu A, Kayala MA, Burk C, Molina DM, et al. Sterile protective immunity to malaria is associated with a panel of novel P. falciparum antigens. Mol Cell Proteomics. 2011; 10:M111 007948.
23. Doolan DL, Mu Y, Unal B, Sundaresh S, et al. Profiling humoral immune responses to P. falciparum infection with protein microarrays. Proteomics. 2008; 8:4680–4694. [PubMed: 18937256]
24. Long AD, Mangalam HJ, Chan BY, Tolleri L, et al. Improved statistical inference from DNA microarray data using analysis of variance and a Bayesian statistical framework. Analysis of global gene expression in Escherichia coli K12. J Biol Chem. 2001; 276:19937–19944. [PubMed: 11259426]
25. Baldi P, Long AD. A Bayesian framework for the analysis of microarray expression data: regularized t -test and statistical inferences of gene changes. Bioinformatics. 2001; 17:509–519. [PubMed: 11395427]

26. Sundaresh S, Doolan DL, Hirst S, Mu Y, et al. Identification of humoral immune responses in protein microarrays using DNA microarray data analysis techniques. Bioinformatics. 2006; 22:1760–1766. [PubMed: 16644788]
27. Sundaresh S, Randall A, Unal B, Petersen JM, et al. From protein microarrays to diagnostic antigen discovery: a study of the pathogen Francisella tularensis. Bioinformatics. 2007; 23:i508–i518. [PubMed: 17646338]
28. Benjamini Y, Hochberg Y. Controlling the false discovery rate: a practical and powerful approach to multiple testing. J Roy Stat Soc, B. 1995; 57:289–300.
29. Liang L, Doskaya M, Juarez S, Caner A, et al. Identification of potential serodiagnostic and subunit vaccine antigens by antibody profiling of toxoplasmosis cases in Turkey. Mol Cell Proteomics. 2011; 10:M110.006916.
30. Hinds S, Myrskog S, Levina L, Koleilat G, et al. NIR-emitting colloidal quantum dots having 26% luminescence quantum yield in buffer solution. J Am Chem Soc. 2007; 129:7218–7219. [PubMed: 17503821]
31. Fernee MJ, Thomsen E, Jensen P, Rubinsztein-Dunlop H. Highly efficient luminescence from a hybrid state found in strongly quantum confined PbS nanocrystals. Nanotechnology. 2006; 17:956–962. [PubMed: 21727366]
32. Wang XY, Qu LH, Zhang JY, Peng XG, Xiao M. Surface-related emission in highly luminescent CdSe quantum dots. Nano Letters. 2003; 3:1103–1106.
33. Talapin DV, Mekis I, Gotzinger S, Kornowski A, et al. CdSe/CdS/ZnS and CdSe/ZnSe/ZnS core-shell-shell nanocrystals. Journal of Physical Chemistry B. 2004; 108:18826–18831.
34. Xu S, Kumar S, Nann T. Rapid synthesis of high-quality InP nanocrystals. J Am Chem Soc. 2006; 128:1054–1055. [PubMed: 16433503]
35. Clapp AR, Pons T, Medintz IL, Delehanty JB, et al. Two-photon excitation of quantum-dot-based fluorescence resonance energy transfer and its applications. Adv Mater. 2007; 19:1921.
36. He GS, Yong KT, Zheng Q, Sahoo Y, et al. Multi-photon excitation properties of CdSe quantum dots solutions and optical limiting behavior in infrared range. Opt Express. 2007; 15:12818–12833. [PubMed: 19550551]
37. Larson DR, Zipfel WR, Williams RM, Clark SW, et al. Water-soluble quantum dots for multiphoton fluorescence imaging in vivo. Science. 2003; 300:1434–1436. [PubMed: 12775841]
38. Young SH, Rozengurt E. Qdot nanocrystal conjugates conjugated to bombesin or ANG II label the cognate G protein-coupled receptor in living cells. American journal of physiology Cell physiology. 2006; 290:C728–732. [PubMed: 16236822]
39. Soper SA, Mattingly QL. Steady-State and Picosecond Laser Fluorescence Studies of Nonradiative Pathways in Tricarbocyanine Dyes - Implications to the Design of near-Ir Fluorochromes with High Fluorescence Efficiencies. Journal of the American Chemical Society. 1994; 116:3744–3752.

Statement of significance

Accessibility of protein microarray worldwide is limited by the lack of a deployable protein microarray imaging system. Here we observed that Qdot detection provides equivalent data to that obtained using conventional organic dye detection. The small portable imager that can be used together with Qdot offers a robust, economical and deployable alternative to conventional laser array scanners that are more costly, fragile and less portable. This can provide new opportunities to individual labs that have difficulty shipping samples out of their countries to protein array core labs or wishing to probe and analyze their own microarrays independently. This is our first step toward applying Qdot in protein microarray applications. We anticipate Qdot will provide increased benefit due to their long luminescence stability, high brightness and multiplex detections.

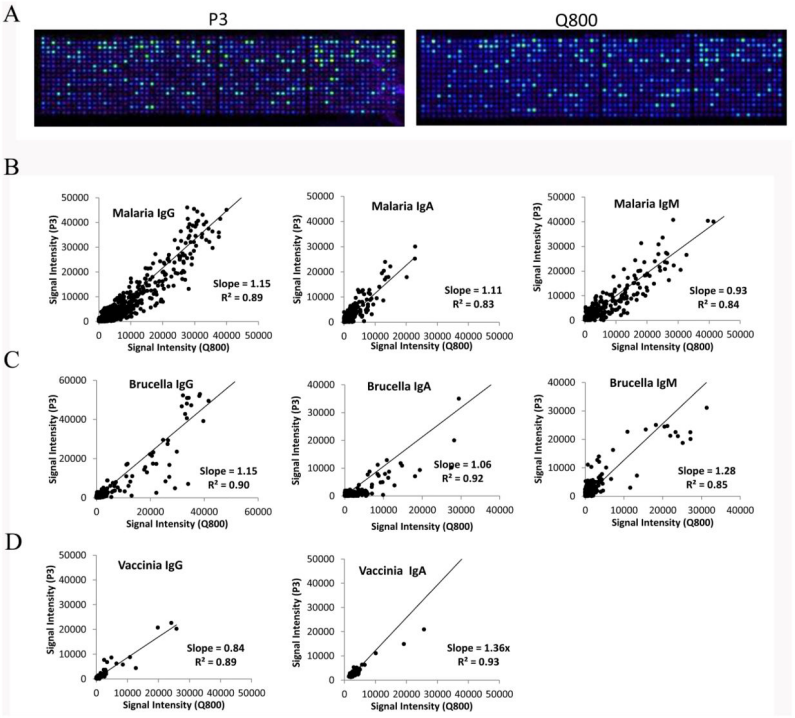

Figure 1.

Comparison of Qdot immunofluorescence and organic fluorescence dye.

(A) Representative image of a Pf1000 array probed with a single Kenyan malaria patient's sample using P3 (left) or Qdot as detection fluorophore. Arrays were quantified using ScanArrayExpress software. Optimal and equivalent Scanning settings for both scanners have been used. Shown in the scatter plots are representative data generated for IgG, IgA, and IgM. Data plotted were raw values with *E.coli* background signals subtracted. (B) Representative image of a Pf1000 array probed with samples from *Pf* exposed individuals in Kalifabougou, Mali. (C) Representative image of a Brucella array probed with a blood culture-positive Brucellosis patient sample. (D) Representative image of a VACV-WR array probed with samples from a Lister-vaccinated individual. Values from the conventional GenePix® scanner are on the y-axis, and the data from the ArrayCam™ on the x-axis. Each dot is an individual protein on the array. Data for 15 samples tested for IgG, IgA and IgM, using arrays for *Plasmodium falciparum*, *Brucella melitensis* and vaccinia virus, are shown in table 1.

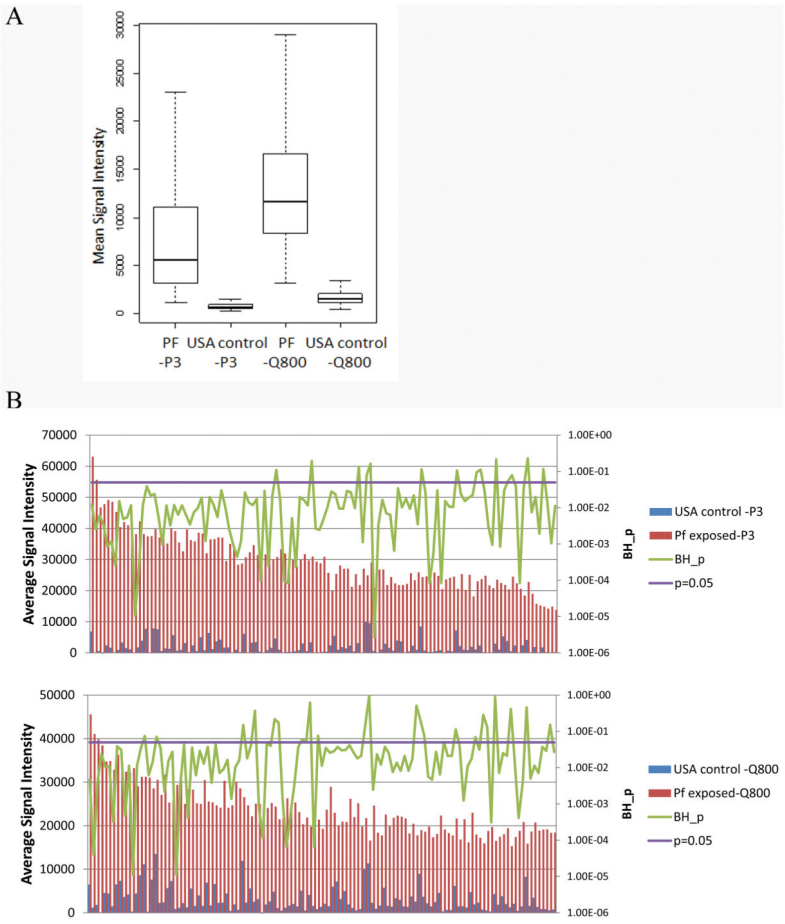

Figure 2.

Differentially reactive antigens distinguishing malaria infection from healthy controls identified using organic P3 or Qdot fluorophores.

(A) Distribution of mean antibody levels in *Pf* exposed individuals and USA controls for 1087 antigens using P3 or Qdot fluorophores. Upper whiskers represent highest values within 1.5 times of inter-quartile range. Lower whiskers represent lowest values in different groups. Outlier values are not shown.

(B) Top 100 reactive antigens were selected from each detection method, with 119 antigens in total. The mean IgG reactivity of the antigens was compared between the *P.falciparum* exposed patients and USA healthy controls for P3 or Qdot fluorophores. Benjamini Hochberg corrected p-values from normalized data are plotted on secondary Y axis. The full list of 119 top reactive antigens is shown in Supplementary table 1.

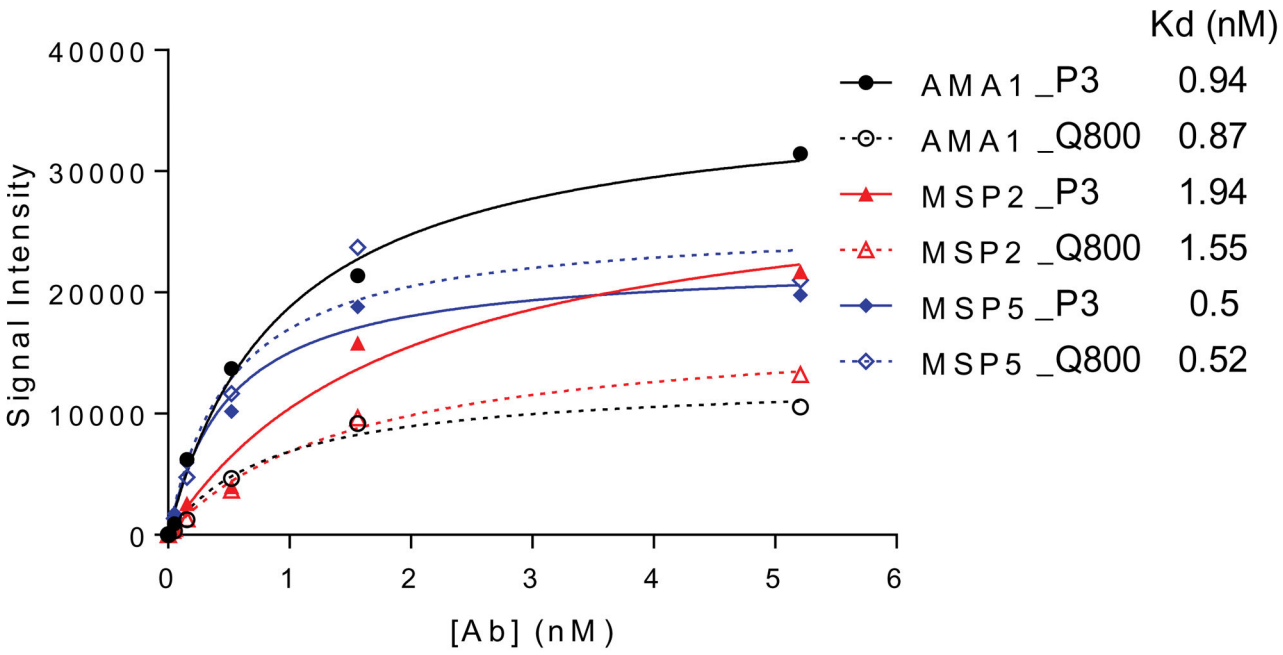

Figure 3.

Comparison of P3 or Qdot platforms for antibody binding kinetics by protein microarray. Anti -*P. falciparum* (*Pf*) monoclonal antibody AMA1 and rabbit anti-sera for Pf MSP2 and MSP5 were titrated and probed on separate Pf1000 arrays. Biotinylated anti-mouse and anti-rabbit secondary antibodies were then used for detection, followed by either P3 or Qdot -conjugated streptavidin-tertiary reagents. Arrays were quantified using ScanArrayExpress software. The results were analyzed using the one-site specific binding model (Graphpad Prism Software) for generation of dissociation constants (Kd) from titrations curves.

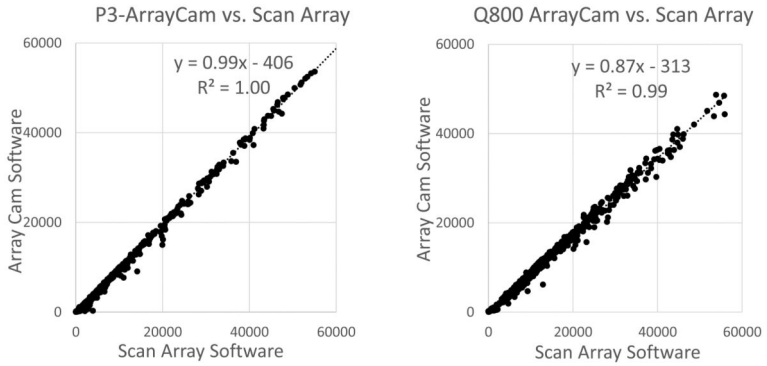

Figure 4.

ScanArrayExpress® and ArrayCam™ data acquisition software comparison. Scatterplots comparing data generated from both software used for quantifying the same images. (A) The same P3 .tiff image generated from GenePix® scanner was quantified using both software suites (B) The same Q800 .tiff image generated from ArrayCam™ scanner was quantified using both software suites.

Table 1

Comparison of Qdot immunofluorescence and organic fluorescence dye (P3) on all samples probed. Data were obtained as described in Fig 1.

P3 vs Q800		Malaria							Brucella			Vaccinia				
		Kali05	**Kali18**	**Kali20**	**PNG40**	**PNG62**	**Kenya73**	**Kenya43**	**#6**	**#8**	**#12**	**pt20 d21**	**pt20 m6**	**pt20 y1**	**pt21 d21**	**pt21 m6**
IgG	Slope	1.15	1.27	0.98	1.24	1.34	1.19	1.1	1.15	1.29	2.06	1.19	0.84	0.88	1.02	0.88
	R^2	0.89	0.84	0.85	0.87	0.86	0.83	0.83	0.9	0.67	0.78	0.78	0.89	0.85	0.87	0.82
IgA	Slope	0.93	1.11	0.85	0.83	1.35	0.64	0.87	1.06	0.61	N/A	1.36	1.59	N/A	0.98	N/A
	R^2	0.78	0.83	0.7	0.7	0.66	0.72	0.79	0.92	0.8		0.93	0.73		0.64	
IgM	Slope	0.93	0.91	0.8	0.81	1.2	0.83	1.15	0.9	1.28	1.34	N/A	N/A	N/A	N/A	N/A
	R^2	0.84	0.59	0.83	0.86	0.82	0.81	0.86	0.59	0.85	0.62					